Multistatic Imaging of Extended Targets

Josselin Garnier (Université Paris Diderot)
http://www.josselin-garnier.org/

Habib Ammari (ETH Zürich), Josselin Garnier (Université Paris Diderot), Hyeonbae Kang (Inha University, Korea), Mikyoung Lim (KAIST, Korea), and Knut Sølna (UC Irvine), SIAM J. Imaging Sci., Vol. 5, pp. 564-600 (2012).

- Sensor array imaging.
- Introduce iterative approaches for imaging extended inclusions from far field measurements.
- Study stability and resolution analysis (with measurement noise).

The array response matrix

- Time-harmonic 2D wave equation with point source:
$$\nabla_{\boldsymbol{x}} \cdot \Big(\frac{1}{\mu(\boldsymbol{x})} \nabla_{\boldsymbol{x}} \hat{u}(\boldsymbol{x}, \boldsymbol{y}) \Big) + \omega^2 \varepsilon(\boldsymbol{x}) \hat{u}(\boldsymbol{x}, \boldsymbol{y}) = -\frac{1}{\mu_0} \delta_{\boldsymbol{y}}(\boldsymbol{x})$$

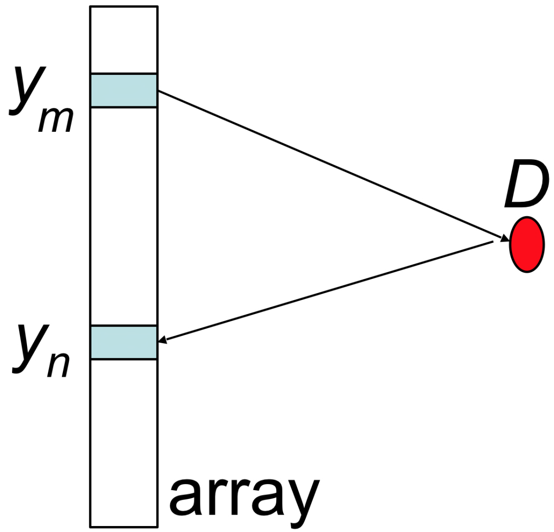

- Array of N elements $\{\boldsymbol{y}_1, \dots, \boldsymbol{y}_N\}$.

- $\hat{u}(\boldsymbol{y}_n, \boldsymbol{y}_m)$ = field recorded by the sensor at $\boldsymbol{y}_n$ when the sensor at $\boldsymbol{y}_m$ emits a time-harmonic signal at frequency ω.

- In the presence of an inclusion $D_{\rm true}$:

$$\mu(\boldsymbol{x}) = \mu_0 \mathbf{1}_{D^c_{\rm true}}(\boldsymbol{x}) + \mu \mathbf{1}_{D_{\rm true}}(\boldsymbol{x}), \qquad \varepsilon(\boldsymbol{x}) = \varepsilon_0 \mathbf{1}_{D^c_{\rm true}}(\boldsymbol{x}) + \varepsilon \mathbf{1}_{D_{\rm true}}(\boldsymbol{x}).$$

Here

- μ_0 (magnetic permeability) and ε_0 (electrical permittivity) are the known background parameters,

- $D_{\rm true}$ is the unknown compactly supported domain with size larger than the wavelength $\lambda_0 = 2\pi/k_0$, $k_0 = \omega/c_0$, $c_0 = 1/\sqrt{\varepsilon_0 \mu_0}$,

- μ and ε are the known inclusion parameters.

The array response matrix

- Multi-static response matrix $\mathbf{A} = (A_{nm})_{n,m=1}^{N}$:

$$A_{nm} = \hat{u}(\boldsymbol{y}_n, \boldsymbol{y}_m) - \hat{G}_0(\boldsymbol{y}_n, \boldsymbol{y}_m) + W_{nm},$$

where
- $\hat{u}(\boldsymbol{y}_n, \boldsymbol{y}_m)$ the field recorded by the sensor at $\boldsymbol{y}_n$ when the sensor at $\boldsymbol{y}_m$ emits,
- $\hat{G}_0(\boldsymbol{y}_n, \boldsymbol{y}_m)$ is the incident field:

$$\hat{G}_0(\boldsymbol{x}, \boldsymbol{y}) = \frac{i}{4} H_0^{(1)}\big(k_0|\boldsymbol{x} - \boldsymbol{y}|\big),$$

- W_{nm} represents measurement noise ($(W_{nm})_{n,m=1}^{N}$ are independent and identically distributed zero-mean random variables).

By reciprocity $\mathbf{A}$ is complex symmetric in the absence of measurement noise.
Symmetrize the matrix $(\mathbf{A} + \mathbf{A}^T)/2$ in the presence of measurement noise.

First imaging algorithm

• Assume we measure $\mathbf{A}_{\text{meas}}$ and we can compute the MSR matrix $\mathbf{A}[D]$ associated with the inclusion D.

• Standard least-square algorithm to image the inclusion: minimize over D in the class of $\mathcal{C}^1$-curves (for ∂D) the cost functional defined by

$$\mathcal{J}_1[D] := \frac{1}{2} \sum_{n,m=1}^{N} \left| A_{nm}[D] - A_{\text{meas},nm} \right|^2 \quad \big(+ \text{Reg}(D) \big).$$

(perimeter regularization [Ben Ameur et al, 2004], total variation regularization [Chan and Tai, 2003, 2004], ...).

• Two critical questions:
- weighting of the least square functional (appropriate weights adapted to the sensor array and to the inclusion).
- representation of the domain D (appropriate parametrization of the boundary ∂D, adapted to the sensor array and to the inclusion).

Second imaging algorithm

- Let $\sigma_{\text{meas}}^{(l)}$, $l = 1, \ldots, N$, be the singular values of $\mathbf{A}_{\text{meas}}$ counted according to multiplicity and $\boldsymbol{v}_{\text{meas}}^{(l)}$ be the singular vector associated with $\sigma_{\text{meas}}^{(l)}$.

Here we use the symmetric Singular Value Decomposition (SVD) of a symmetric complex matrix $\mathbf{A} = \mathbf{V}\boldsymbol{\Sigma}\overline{\mathbf{V}}^T$.

- Minimize over D the cost functional defined by

$$\mathcal{J}_2[D] := \frac{1}{2}\sum_{l=1}^{L} W(\sigma_{\text{meas}}^{(l)}) \left\| \left(\mathbf{A}[D] - \mathbf{A}_{\text{meas}}\right)\boldsymbol{v}_{\text{meas}}^{(l)} \right\|^2$$

with $L \leq N$ and W a weight (nonnegative) function.

- Use an iterative method. We need:

- an initial guess D_0,
- an update procedure $D_j \to D_{j+1}$.

Initial guess

- Use

$$\mathcal{I}_{\mathrm{RT}}(\boldsymbol{x}) = \overline{\boldsymbol{g}(\boldsymbol{x})}^{T} \mathbf{A}_{\mathrm{meas}} \overline{\boldsymbol{g}(\boldsymbol{x})},$$

with

$$\boldsymbol{g}(\boldsymbol{x}) = \Big(\frac{\exp(ik_0 |\boldsymbol{x} - \boldsymbol{y}_n|)}{\sqrt{N}} \Big)_{n=1}^{N}.$$

$\hookrightarrow$ Determine center (argmax of $\mathcal{I}_{\mathrm{RT}}$) and equivalent disk of the inclusion.

Remark: Bayesian analysis shows that it is the optimal method (for minimizing the localization error) in the presence of measurement noise.

Shape derivatives

- The shape derivative of a functional $\mathcal{J}[D]$ is

$$(d_{\mathcal{S}}\mathcal{J}[D], h) = \lim_{\delta \to 0} \frac{\mathcal{J}[D^{\delta h}] - \mathcal{J}[D]}{\delta},$$

where $\partial D^{\delta h} := \{\boldsymbol{x} + \delta h(\boldsymbol{x})\boldsymbol{\nu}(\boldsymbol{x}), \boldsymbol{x} \in \partial D\}$, $\boldsymbol{\nu}(\boldsymbol{x})$ is the outward unit normal to ∂D, and h is a $\mathcal{C}^1$ function on ∂D.

- Examples of D^h for $D = \{\boldsymbol{x} = r(\cos\theta, \sin\theta),\ r \leq 1,\ \theta \in [0, 2\pi]\}$:

$$D^h = \{\boldsymbol{x} = r(\cos\theta, \sin\theta),\ r \leq 1 + h(\theta),\ \theta \in [0, 2\pi]\}$$

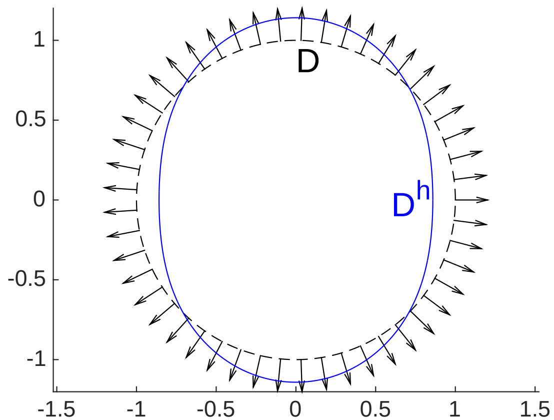

$h(\theta) = -0.15\cos(2\theta)$

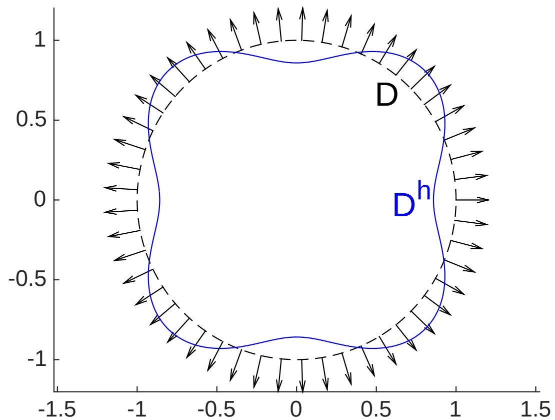

$h(\theta) = -0.15\cos(4\theta)$

Shape derivatives

- The shape derivative of a functional $\mathcal{J}[D]$ is

$$(d_{\mathcal{S}}\mathcal{J}[D], h) = \lim_{\delta \to 0} \frac{\mathcal{J}[D^{\delta h}] - \mathcal{J}[D]}{\delta},$$

where $\partial D^{\delta h} := \big\{ \boldsymbol{x} + \delta h(\boldsymbol{x})\boldsymbol{\nu}(\boldsymbol{x}), \boldsymbol{x} \in \partial D \big\}$, $\boldsymbol{\nu}(\boldsymbol{x})$ is the outward unit normal to ∂D, and h is a $\mathcal{C}^1$ function on ∂D.

- Expansion for small perturbation δh:

$$A_{nm}[D^{\delta h}] - A_{nm}[D] = \delta \int_{\partial D} h(\boldsymbol{x}) B_{nm}[D](\boldsymbol{x}) d\sigma(\boldsymbol{x}) + o(\delta),$$

where

$$\begin{aligned} B_{nm}[D](\boldsymbol{x}) \quad := \quad & \nabla_{\boldsymbol{x}} u[D](\boldsymbol{x}, \boldsymbol{y}_n)^T \mathbf{M}[\frac{\mu_0}{\mu}](\boldsymbol{x}) \nabla_{\boldsymbol{x}} u[D](\boldsymbol{x}, \boldsymbol{y}_m) \\ & + \omega^2 (\varepsilon - \varepsilon_0) \mu_0 u[D](\boldsymbol{x}, \boldsymbol{y}_n) u[D](\boldsymbol{x}, \boldsymbol{y}_m), \end{aligned}$$

$\mathbf{M}$ is the polarization tensor

$$\mathbf{M}[\frac{\mu_0}{\mu}](\boldsymbol{x}) = \big(\frac{\mu_0}{\mu} - 1\big) \Big(\frac{\mu_0}{\mu} \boldsymbol{\nu}(\boldsymbol{x}) \otimes \boldsymbol{\nu}(\boldsymbol{x}) + \boldsymbol{\tau}(\boldsymbol{x}) \otimes \boldsymbol{\tau}(\boldsymbol{x}) \Big), \quad \boldsymbol{x} \in \partial D,$$

and $\boldsymbol{\tau}(\boldsymbol{x})$ is the unit tangential vector to ∂D at $\boldsymbol{x}$.
Note that the matrix $\mathbf{B}$ is a propagator.

• For the two cost functionals:

$$
\begin{aligned}
(d_{\mathcal{S}}\mathcal{J}_1[D], h) &= \sum_{n,m=1}^{N} \mathrm{Re}\Big[\big(A_{nm}[D] - A_{\mathrm{meas},nm}\big) \int_{\partial D} h(\boldsymbol{x}) \overline{B_{nm}[D](\boldsymbol{x})}\, d\sigma(\boldsymbol{x})\Big], \\
(d_{\mathcal{S}}\mathcal{J}_2[D], h) &= \mathrm{Re} \sum_{l=1}^{L} W(\sigma_{\mathrm{meas}}^{(l)}) \int_{\partial D} h(\boldsymbol{x}) \Big\langle (\mathbf{A}[D] - \mathbf{A}_{\mathrm{meas}}) \boldsymbol{v}_{\mathrm{meas}}^{(l)},\, \mathbf{B}[D](\boldsymbol{x}) \boldsymbol{v}_{\mathrm{meas}}^{(l)} \Big\rangle d\sigma(\boldsymbol{x}).
\end{aligned}
$$

• Therefore, we look for the perturbation h in the vector spaces spanned by $\{\psi_p\}_{p=1}^{P}$:

$$
\begin{aligned}
&\text{Algo 1:} \quad \{\psi_p\}_{p=1}^{P} = \{\mathrm{Re}(B_{nm}[D])\}_{n,m=1}^{N} \cup \{\mathrm{Im}(B_{nm}[D])\}_{n,m=1}^{N}, \\
&\text{Algo 2:} \quad \{\psi_p\}_{p=1}^{P} = \{\mathrm{Re}\langle (\mathbf{A}[D] - \mathbf{A}_{\mathrm{meas}}) \boldsymbol{v}_{\mathrm{meas}}^{(l)},\, \mathbf{B}[D] \boldsymbol{v}_{\mathrm{meas}}^{(l)} \rangle\}_{l=1}^{L}.
\end{aligned}
$$

• For Algo 2:

• Use special propagated illuminations as a basis for the perturbation h (special regularization).

• Given ∂D_j, compute $\partial D_{j+1} := \partial D_j^{h_j}$ by applying the gradient descent method, where $\partial D_j^{h_j} := \{\boldsymbol{x} + h_j(\boldsymbol{x})\boldsymbol{\nu}(\boldsymbol{x}), \boldsymbol{x} \in \partial D_j\}$ and:

$$
h_j(\boldsymbol{x}) = -\frac{\mathcal{J}_m[D_j]}{\sum_{l=1}^{L} |(d_{\mathcal{S}}\mathcal{J}_m[D_j], \psi_l)|^2} \sum_{l=1}^{L} (d_{\mathcal{S}}\mathcal{J}_m[D_j], \psi_l)\, \psi_l .
$$

(use Armijo's rule [Nocedal and Wright, 1999] if $\mathcal{J}_m[D_{j+1}] > \mathcal{J}_m[D_j]$).

Resolution and stability analysis

- Resolution and stability are dependent.
- Assume $D_{\rm true}$ is a slightly perturbed disk:

$$D_{\rm true} = \{\boldsymbol{x} = r(\cos\theta, \sin\theta),\ r \leq r_0 + h_{\rm true}(\theta),\ \theta \in [0, 2\pi]\}, \qquad h_{\rm true}(\theta) = \sum_{p=-\infty}^{\infty} \hat{h}_{{\rm true},p} e^{ip\theta},$$

the contrast is small, and the transducers are densely sampled at the surface a disk with large radius (full and continuous aperture).

- With measurement noise, Algo 1 gives unbiased estimation of $\hat{h}_{{\rm true},p}$ with the variance

$$\mathrm{Var}(\hat{h}_{{\rm est},p}) = \frac{r_0^2\sigma^2}{4\sum_{l=-\infty}^{\infty} J_l^2(k_0r_0)J_{p-l}^2(k_0r_0)}.$$

- From the behavior of $\Psi(p) := \sum_{l=-\infty}^{\infty} J_l^2(k_0r_0)J_{p-l}^2(k_0r_0)$: the estimation of $\hat{h}_{{\rm true},p}$ is possible for $p < 2k_0r_0$ and impossible for $p > 2k_0r_0$.
- The coefficient $\hat{h}_{{\rm true},p}$ corresponds to a characteristic length scale $2\pi r_0/p$.

$\hookrightarrow$ the limitation $p < 2k_0r_0$ corresponds to a length scale larger than half a wavelength (diffraction limit).

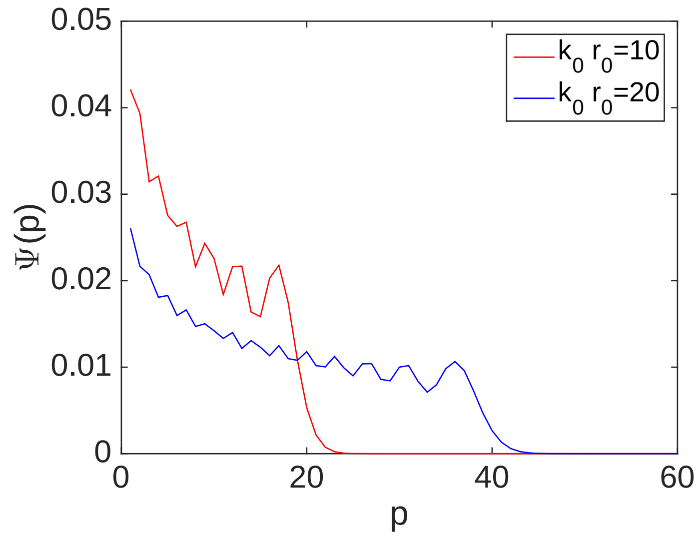

Resolution and stability analysis

- General results with full aperture, star-shaped obstacles:

- $\sigma_{\rm meas}^{(l)}$ is large for $l < N_{\rm meas}$, with $N_{\rm meas} \sim |\partial D_{\rm true}|/\lambda_0$; the corresponding propagated singular vectors are supported on the main reflective parts of ∂D and are low-frequency,
- $\sigma_{\rm meas}^{(l)}$ plunges to zero for l in a transition region around $N_{\rm meas}$; the corresponding propagated singular vectors are supported at the edges of ∂D and are high-frequency,
- $\sigma_{\rm meas}^{(l)}$ is small for $l > N_{\rm meas}$.

- Similar results with partial aperture:

The propagated singular vectors in the transition region are supported at the edges of the domain.
Example: for a linear array, the singular vectors correspond to the ones of the sinc kernel (prolate spheroidal functions) [Borcea et al, SIIMS 2008].

$\hookrightarrow$ By choosing large weights for the singular values/vectors in the transition region, one can enhance the illumination of the edges of the inclusion.

Numerical illustrations

- Set up: 20 transducers at the surface of the disk with radius 10, $\omega = 2$, $\lambda_0 = \pi$.

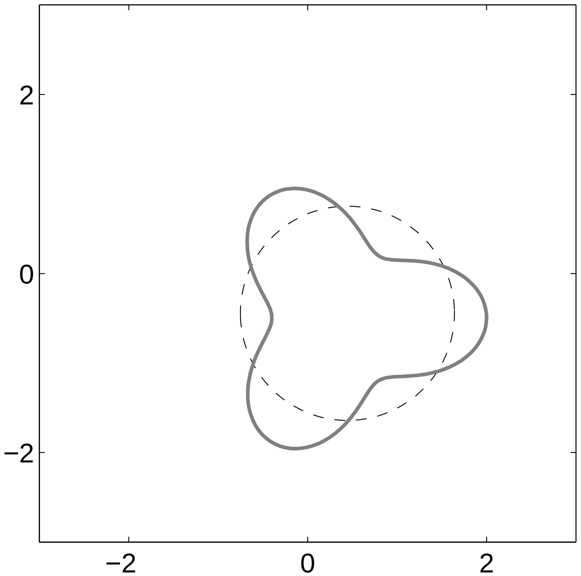

True inclusion
and initial guess

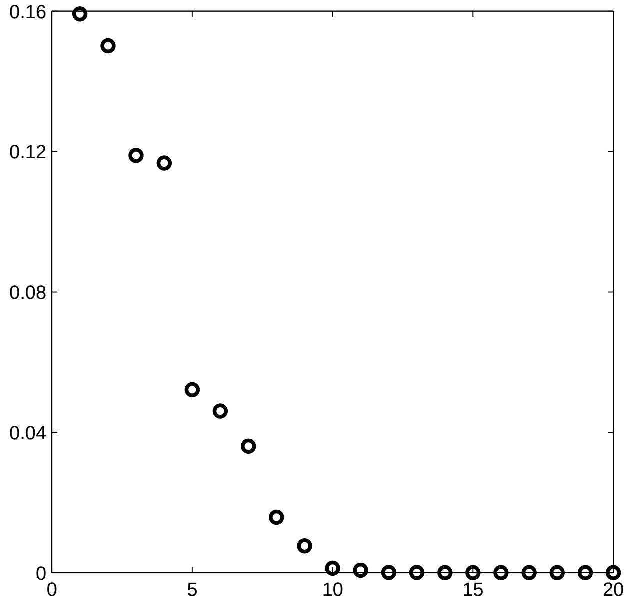

Singular values
of the true MSR matrix

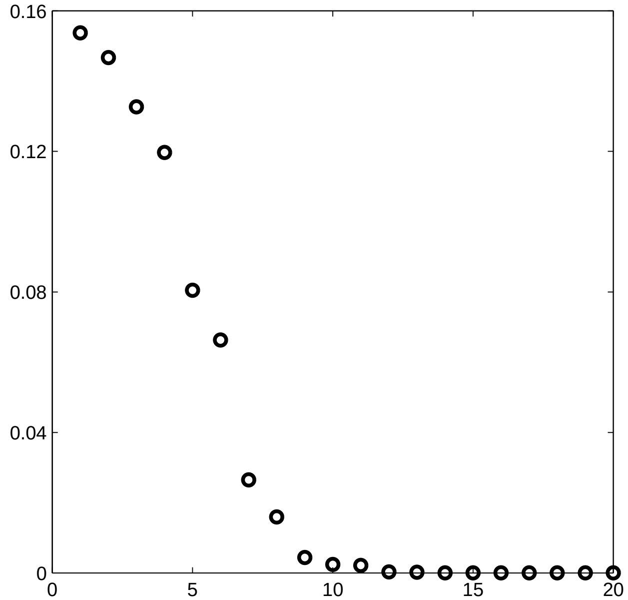

Singular values
of the MSR matrix of the disk

- Choice of the weights for Algo 2: The weights are taken successively as follows:
  - $W(\sigma_{\text{meas}}^{(l)}) = 1$ for $1 \leq l \leq 5$ and 0 elsewhere,
  - $W(\sigma_{\text{meas}}^{(l)}) = 1$ for $6 \leq l \leq 10$ and 0 elsewhere,
  - $W(\sigma_{\text{meas}}^{(l)}) = 1$ for $1 \leq l \leq 10$ and 0 elsewhere.

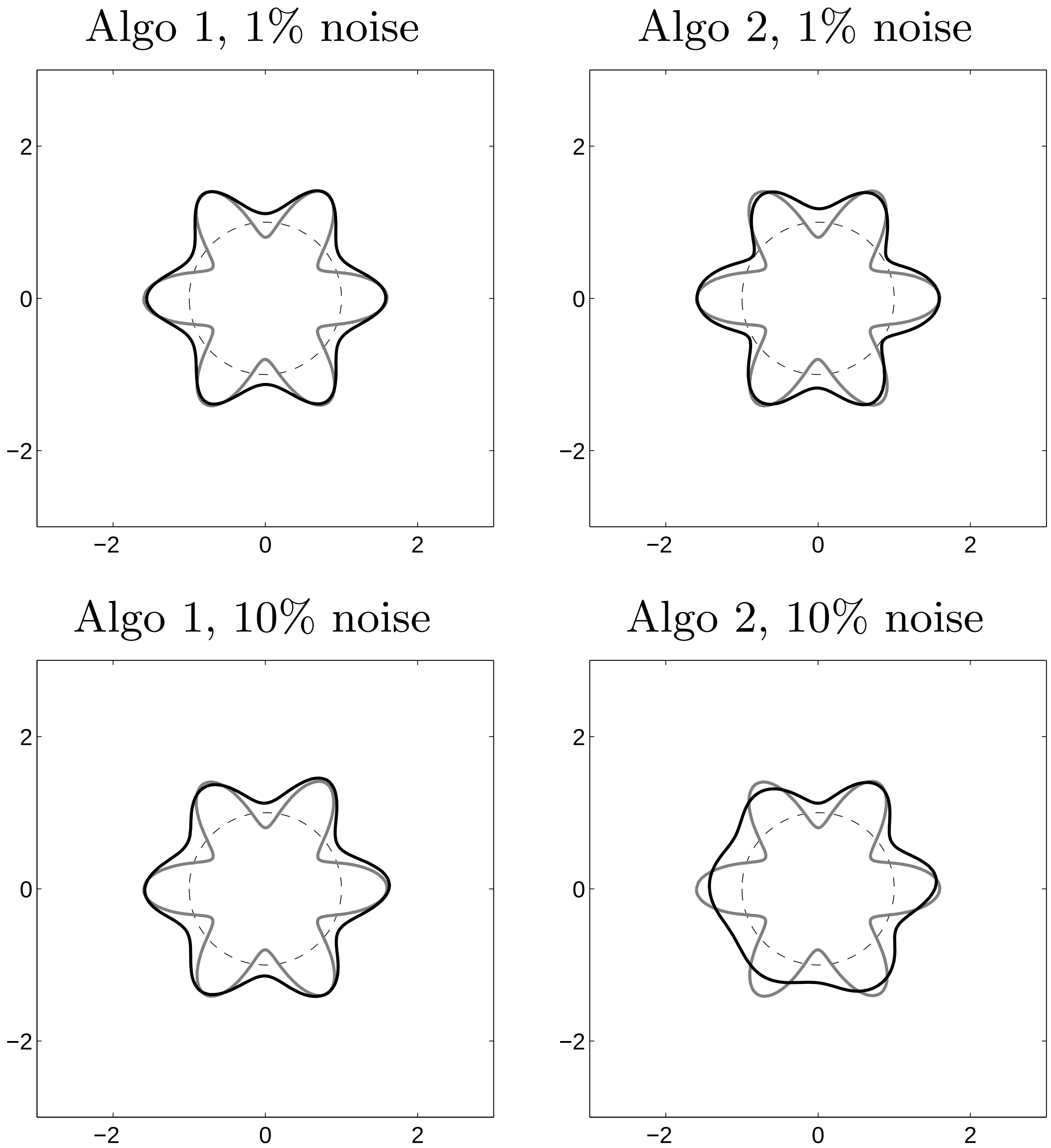

Here $\omega = 2$, $\lambda_0 = \pi$, and full aperture array (20 transducers at the surface of the disk with radius 10).

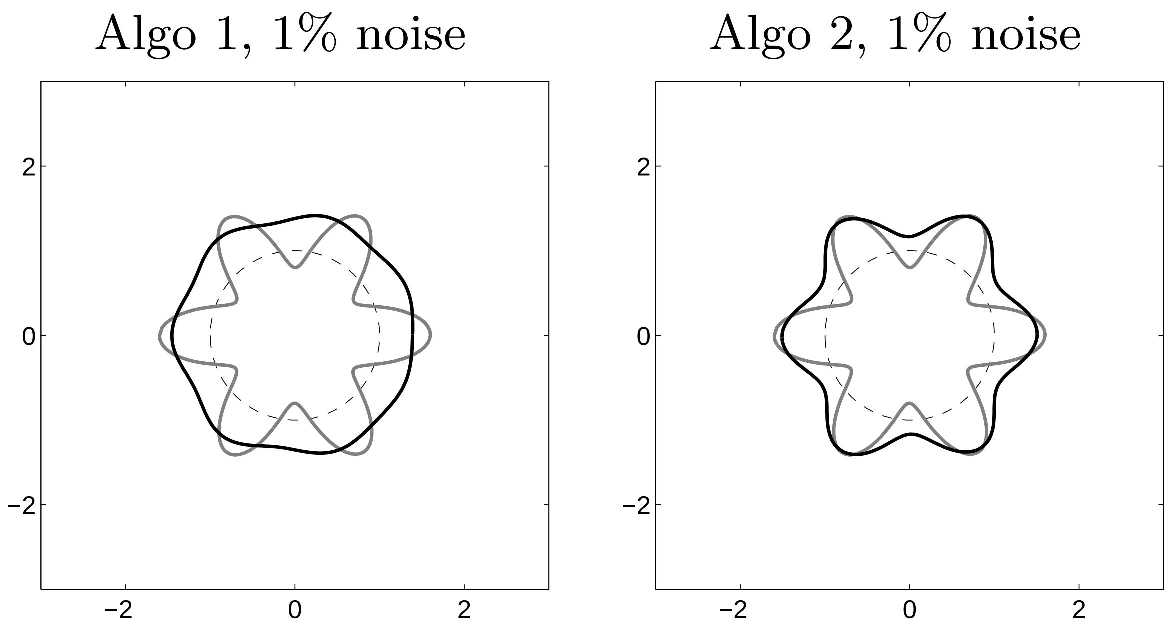

Here $\omega = 1$, $\lambda_0 = 2\pi$, and full aperture array (20 transducers at the surface of the disk with radius 10).

- Algo 2 can detect (highly compared to the wavelength) oscillatory boundary perturbations which are undetectable with Algo 1.

- Algo 2 is more sensitive to measurement noise than Algo 1.

Extension: A third algorithm

- Cost functional at step j:

$$\mathcal{J}_3^{(j)}[D_j+\delta D] := \frac{1}{2}\sum_{l'=1}^{L'}\sum_{l=1}^{L} W(\sigma^{(l)}_{\mathrm{meas}})\, W'(\sigma^{(l')}[D_j]) \left|\Big\langle (\mathbf{A}[D_j+\delta D]-\mathbf{A}_{\mathrm{meas}})\boldsymbol{v}^{(l)}_{\mathrm{meas}}, \boldsymbol{v}^{(l')}[D_j]\Big\rangle\right|^2.$$

- Shape derivative:

$$\begin{aligned}(d_{\mathcal{S}}\mathcal{J}_3^{(j)}[D_j],h) \quad &= \quad \mathrm{Re}\sum_{l'=1}^{L'}\sum_{l=1}^{L} W(\sigma^{(l)}_{\mathrm{meas}})W'(\sigma^{(l')}[D_j]) \Big\langle (\mathbf{A}[D_j]-\mathbf{A}_{\mathrm{meas}})\boldsymbol{v}^{(l)}_{\mathrm{meas}},\ \boldsymbol{v}^{(l')}[D_j]\Big\rangle \\ &\times \int_{\partial D} h(\boldsymbol{x})\overline{\Big\langle \mathbf{B}[D_j](\boldsymbol{x})\boldsymbol{v}^{(l)}_{\mathrm{meas}}\ ,\ \boldsymbol{v}^{(l')}[D_j]\Big\rangle} d\sigma(\boldsymbol{x}).\end{aligned}$$

- Representation basis for the perturbation h at step j:

$$\{\psi_p\} = \{\mathrm{Re}\langle \mathbf{B}[D_j]\boldsymbol{v}^{(l)}_{\mathrm{meas}}\ ,\ \boldsymbol{v}^{(l')}[D_j]\rangle\} \cup \{\mathrm{Im}\langle \mathbf{B}[D_j]\boldsymbol{v}^{(l)}_{\mathrm{meas}}\ ,\ \boldsymbol{v}^{(l')}[D_j]\rangle\}.$$

Conclusions

- Original iterative optimization algorithms to recover the shape of an inclusion using a multi-static response matrix.

- Backpropagating the singular vectors provides a natural basis for computing the shape perturbation at each step.

- Increasing the weights of the contributions of the singular values/vectors in the transition region enhances the illumination of the edges and allows to increase resolution slightly beyond diffraction limit.

- Extensions:

- multiple frequencies (hopping algorithm).
- elastic case.
- level-set reconstruction algorithm.

Conclusions

- Original iterative optimization algorithms to recover the shape of an inclusion using a multi-static response matrix.

- Backpropagating the singular vectors provides a natural basis for computing the shape perturbation at each step.

- Increasing the weights of the contributions of the singular values/vectors in the transition region enhances the illumination of the edges and allows to increase resolution slightly beyond diffraction limit.

- Extensions:

- multiple frequencies (hopping algorithm).
- elastic case.
- level-set reconstruction algorithm.

See also our more recent work: